

Size effects in the electronic heat capacity of small platinum particles embedded in silica*

G. R. Stewart

Department of Applied Physics, Stanford University, Stanford, California 94305

(Received 30 October 1975)

Heat-capacity measurements on sputtered granular metal films of Pt-SiO₂ were carried out between 1 and 12°K. Mean sizes of the Pt particles range from 10 to 26 Å; this small size coupled with these low temperatures makes the average electronic-energy-level spacing δ in the Pt metal large compared to $k_B T$. A quantum size effect in the electronic heat capacity of a metal has been predicted in this limit, $\delta \gg k_B T$, and is observed here for the first time, although in a very limited temperature range. Difficulty in observing this size effect was caused by a large heat-capacity enhancement over bulk values in the insulating vitreous silica. This enhancement is ascribed to the Pt particle inclusions in the host SiO₂ matrix augmenting the low-frequency Einstein modes first observed in the specific heat of SiO₂ by Flubacher *et al.*

I. INTRODUCTION

This study was to investigate the effects of small size on the electronic heat capacity of a metal. For reasons discussed below, platinum was chosen to be cosputtered with electrically insulating silica. A series of four Pt-SiO₂ samples with median particle sizes ranging from 10 to 26 Å were prepared, and measured from 1 to 12°K with an automated small sample calorimeter.¹ Several theoretical predictions²⁻⁵ had been made on what the heat capacity of small metal particles should be when the level spacing between adjacent electronic energy levels, δ , became much larger than the thermal broadening energy, $k_B T$.

This work is the first to measure a sizable decrease in the heat capacity of an ensemble of small metal particles within an insulating matrix. This decrease is discussed in light of the above-mentioned theories²⁻⁵ of size effects in the electronic heat capacity (C^{el}) of small metal particles. The only other heat-capacity work on isolated small metal particles to date has been by Novotny, Meincke, and Watson,⁶ and by Novotny and Meincke (NM).⁷ Their work was designed to investigate surface phonon effects. In that work, superconducting lead particles 22–60 Å in size were measured, as well as 22-Å In particles. Since the electronic heat capacity (C^{el}) was such a small portion of the total, at most 7% in that work, no opportunity for accurate determination of size effects in C^{el} was present. However, NM⁷ did claim to see some slight [(1–2)%] decrease in C_{Pb} between 5 and 8°K which they ascribed to decreases in $C_{\text{Pb}}^{\text{el}}$. In the present work, C^{el} is greater than 60% of C_{Pt} below 5°K. In the aggregate Pt-SiO₂, C^{el} of the platinum ranges from 50 to 75% of the total C at 1.3°K and from 11 to 14% of the total aggregate C at 5°K for the four samples reported on herein. Thus, the present work has a greatly

enhanced sensitivity to small changes in C^{el} over previous efforts.

II. THEORETICAL BACKGROUND

In order to calculate the heat capacity of a collection of metal particles with discrete electronic energy levels ($\delta \gg k_B T$), it is necessary to know the probability distribution of levels adjacent to the Fermi energy. This type of statistical problem received a great deal of attention, both experimental and theoretical, for the case of nuclear energy levels during the 1950's.⁸ Initially, probability distributions of level spacings were taken to be exponential,

$$P(\delta) \propto e^{-\delta}, \quad (1)$$

i.e., the levels were randomly distributed with respect to one another. This distribution gives a maximum probability for zero level spacing, implying that adjacent energy levels tend to lie close together. However, experiments⁹ showed the direct opposite, that the probability of the adjacent level lying nearby in energy went to zero with the level spacing, δ . This prompted Wigner¹⁰ to propose a new level distribution, now known as the "Wigner surmise,"

$$P(\delta) \propto \delta \exp(-\text{const.} \times \delta^2), \quad (2)$$

which fits the nuclear data rather well.

Following this early work, Dyson¹¹ came forward with a rigorous mathematical treatment of the problem: what is the probability distribution of the eigenvalues of an ensemble of random matrices, constrained to follow certain symmetry properties? It is necessary to consider this type of problem for the small particle case important here, because while a given particle will have a certain well-defined Hamiltonian and therefore certain electronic energy levels; experimentally,

TABLE I. Predictions for the heat capacity of small metal particles in the low-temperature limit.

Results of Kubo (Ref. 4)		
	Orthogonal	$C \propto T^2$
	Symplectic	$C \propto T^5$
	Unitary	$C \propto T^3$
Results of DMS (Ref. 5)		
C/k	even	odd
Poisson	$5.02k_B T/\delta$	$3.29k_B T/\delta$
Orthogonal	$3.02 \times 10(k_B T/\delta)^2$	$1.78 \times 10(k_B T/\delta)^2$
Symplectic	$3.18 \times 10^4(k_B T/\delta)^5$	$1.64 \times 10^4(k_B T/\delta)^5$
Unitary	$5.88 \times 10^2(k_B T/\delta)^3$	

heat capacity can only measure a large ensemble of particles. As long as each of these particles is of the same metal, the important symmetries will be universal, these symmetries being whether the electron's spin is a good quantum number (whether the spin-orbit coupling parameter η is greater or less than the level splitting δ), and whether there is time-reversal invariance (magnetic field μH relative to δ).

This applicability to the small particle case of Dyson's work, built on the nuclear energy-level work of the 1950's, was used by Kubo⁴ and by Denton, Muhlschlegel, and Scalapino (DMS)⁵ to calculate the low-temperature electronic specific heat (C^{el}) of an ensemble of electrically isolated, rough-surfaced small metal particles. For Dyson's three symmetries, called orthogonal ($\eta \ll \delta$; $H=0$), symplectic ($\eta \gg \delta$; $H=0$), and unitary ($\eta \gg \delta$; $\mu H \gg \delta$), Kubo and DMS arrived at the results in Table I, where the results for the three types of metals have distinctly different leading term temperature dependences, all of them different from the usual first power dependence of C^{el} in a bulk metal,

$$C^{\text{el}} = \frac{2}{3} \pi^2 k_B^2 N(0) T = \gamma T. \quad (3)$$

Kubo merely used the single adjacent level to the Fermi level with the Dyson statistics. Thus, his calculation of the leading temperature dependence of C^{el} is applicable only at very low temperatures $k_B T \ll \delta$. DMS used several adjacent levels and found the results in Table I whose validity extends up to $k_B T \approx 0.1\delta$. DMS (see also Denton¹²) in addition showed that their low- T -limit results were dependent on size variance only in the coefficient, not in the power law exponent.

In addition to the temperature dependence, the size of the predicted C^{el} shows marked differences from the bulk. DMS's calculation of C^{el} via computer (see Fig. 1) extends beyond the low T limit of $k_B T \leq 0.1\delta$ and shows a marked decrease in the small particle C^{el} , both from bulk values and from a calculation by Kubo³ using the random level dis-

tribution of Eq. (1). As can be seen in Table I and in Fig. 1, Kubo's early calculation gives a linear temperature dependence but decreased by approximately half below the bulk value. The DMS predictions at very low temperatures can be seen in Fig. 1 to be extremely small relative to the bulk C^{el} , reflecting the decrease in the temperature derivative of the energy of a system where inter-

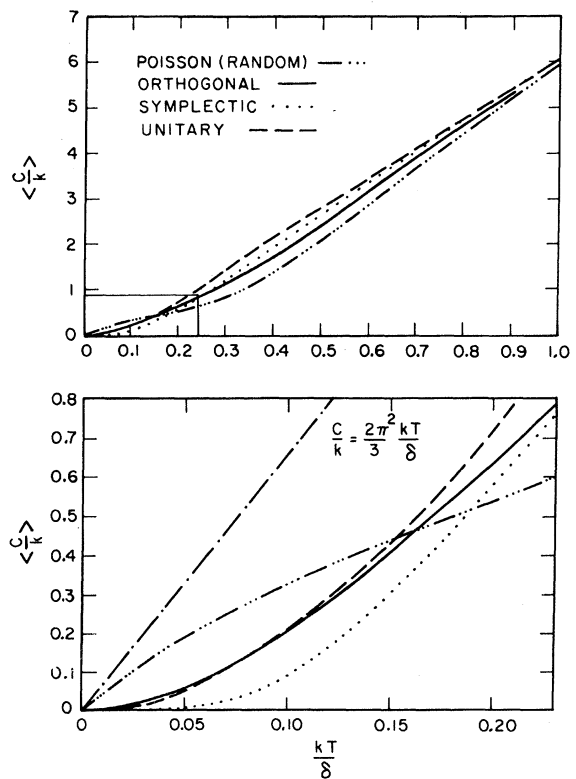


FIG. 1. C^{el} for isolated small metal particles, as calculated by DMS (Ref. 5). Leading term temperature dependences of Table I are valid only below $k_B T/\delta \leq 0.1$ as shown in the expansion of the low-temperature behavior of C .

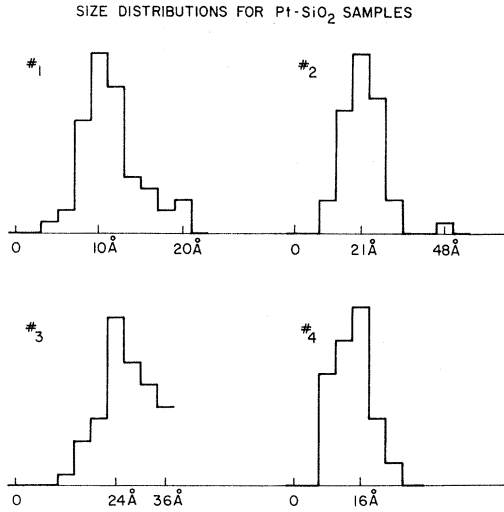


FIG. 2. Histograms of particle sizes in the four Pt-SiO₂ samples. Widths of the distributions are quite small except for a larger particle tail existing in the distribution for sample No. 3, with median particle size of 26 Å.

level thermal excitation is suppressed,

$$C = \frac{\partial E}{\partial T}. \quad (4)$$

III. EXPERIMENTAL METHODS

These predictions of DMS predicate a rigorously constrained experimental design, which fortunately became possible to accomplish using the small sample automated calorimeter developed at Stanford.¹

By cosputtering a small amount of nonreactive metal like Pt or Au with an insulator like Al₂O₃ or SiO₂, it was found feasible to create isolated small metal particles. Substrate temperature, type of metal, amount of metal on the target, and sputtering power were all investigated as ways to vary the particle size. Sputtering at a fixed, low (50-W) power for periods exceeding 100 h using Pt while varying the surface area of metal on the target between production runs was found to produce films with small particles (<30 Å), quite narrow size distributions (see Fig. 2), adequate metal content (>15 wt.%, see Table II), and with sufficient weight (15 mg) of composite metal-insulator in order to measure *C* with reasonable absolute accuracy (better than 5%). Pt gives much smaller particle sizes than Au for the same conditions due to Pt's lower mobility upon arriving at the substrate. This smaller size creates larger level spacing. Using as an approximation⁵

$$\delta \cong \epsilon_F / N, \quad (5)$$

where ϵ_F is the Fermi energy and *N* is the number of electrons in the particle, Fig. 2 and Table II show that the films studied herein are certainly in DMS's limit $k_B T \leq 0.1\delta$ between 1 and 10°K. Alternatively, using the quantum-mechanical particle-in-a-box model for level splitting, Table II shows that the DMS limit is also reached within the range of measurement of this experiment, 1 to 12°K. The choice of SiO₂ over Al₂O₃ was a more difficult decision. Sputtered Al₂O₃ was found to always have a low-temperature Schottky peak in *C*,^{13,14} thus, SiO₂ was used, even though SiO₂ has

TABLE II. Parameters for the four Pt-SiO₂ samples.

	Sample No. 1	Sample No. 2	Sample No. 3	Sample No. 4
Average particle size	10 Å	21 Å	26 Å	16 Å
Sputtering rate (Å/h)	5000	?	7200	3900
Film weight (mg)	15.975	16.21	16.97	16.263
Approximate film thickness (μ)	75	41	112	42
Density (g/cm ³)	1.33	2.04	1.78	4.64
Microprobe run No. 1				
Pt wt.%	17.7%	33.6%	27.9%	16.7%
SiO ₂ wt.%	82.3%	66.4%	72.1%	83.3%
Microprobe run No. 2				
Pt. wt.%	15.6%	32.5%	28.9%	16.0%
SiO ₂ wt.%	84.4%	67.5%	71.1%	84.0%
Heat-capacity addenda				
<i>T</i> =1.25°K	39%	24%	42%	36%
4.2°K	38%	40%	44%	53%
9.2°K	34%	41%	41%	52%
Energy-level splitting				
$\delta/k_B = \epsilon_F/N$	1680°K	176°K	96°K	410°K
Particle in a box				
δ/k_B	1016°K	104°K	57°K	243°K

a larger C than Al_2O_3 , thus obscuring more the metal contribution, has a linear term at low temperatures,^{15,16} and has three Einstein modes¹⁵ at 13, 32, and 58°K that are important contributions to C .

The parameters for the four Pt-SiO₂ films finally used in this study are given in Table II. The particle sizes were determined by transmission electron microscopy (TEM) on thin samples sputtered under identical conditions onto carbon-coated copper grids. As may be seen in Fig. 2, particle size distributions are quite narrow for three of the four films; film No. 3 has a substantial amount of particles larger than the median 26 Å size quoted in Table II. Two different checks were made to ensure that these thin TEM samples were adequate representations of the particle size in the thick samples used for measurement of C . One was to increase the sputtering time of the thin samples from 3 min to 9 and also 15 min. As can be derived from the sputtering rates of Table II, this corresponds to changing the thickness from ≈ 250 to ≈ 1250 Å. TEM photos on this progression of thicknesses show no detectable increase in particle sizes. Another check was to attempt to determine particle size via x-ray line-broadening techniques.¹⁷ Although this technique becomes somewhat uncertain for these very small particle sizes due to complications in the theory,¹⁷ it did serve to further substantiate the sizes shown in Table II for the thick samples, since the x rays sampled the entire film thickness.

Cosputtering a metal with insulator has two definite advantages over the porous glass technique of NM.⁷ One is that the metal particles have excellent thermal contact with the surrounding insulator. Also, determination of particle sizes via TEM presents greater ease and accuracy over the primary techniques of NM, mercury porosimetry, and nitrogen gas adsorption-desorption using the Kelvin equation.⁷ The obvious disadvantage of sputtering is the small yield of material (~ 15 mg) versus the plentiful yield (2–4 g) of NM. This was surmounted by the small sample calorimeter mentioned above.

This calorimeter has a unique thermometer, a small piece (~ 25 mg) of silicon with phosphorous diffused into it. After etching to a depth where the doped phosphorous gives a convenient (1–10 k Ω) resistance at 4°K, a quite sensitive thermometer [$\alpha = (1/R)(dR/dT) = 0.4$] in the range 1–12°K is obtained. The sample to be measured is thermally bonded to the inactive side of the silicon via Wakefield grease. Six 0.0762-mm (3-mil) Au-Cu wires provide mechanical support and electrical contact to the two thermometer sections and a third section with a Cr-Ti heater evaporated onto it. Further

details are given in the literature.^{1,18}

This thermometer plus sample combination then has its temperature response to heat input measured via a Wheatstone bridge driven by a lock-in amplifier. The response of this PAR HR-8 is monitored with a Nicolet 1070 signal-averaging computer, which allows the very fast responses of small samples to be detected from random noise. This relatively noiseless product of repeated averaging is then analyzed via a dedicated PDP-8/e computer. After subtracting addenda corrections, real time C data are printed out. As described in Table II, the addenda for this experiment (known to $\pm 3\%$) were typically less than 40% of the total,

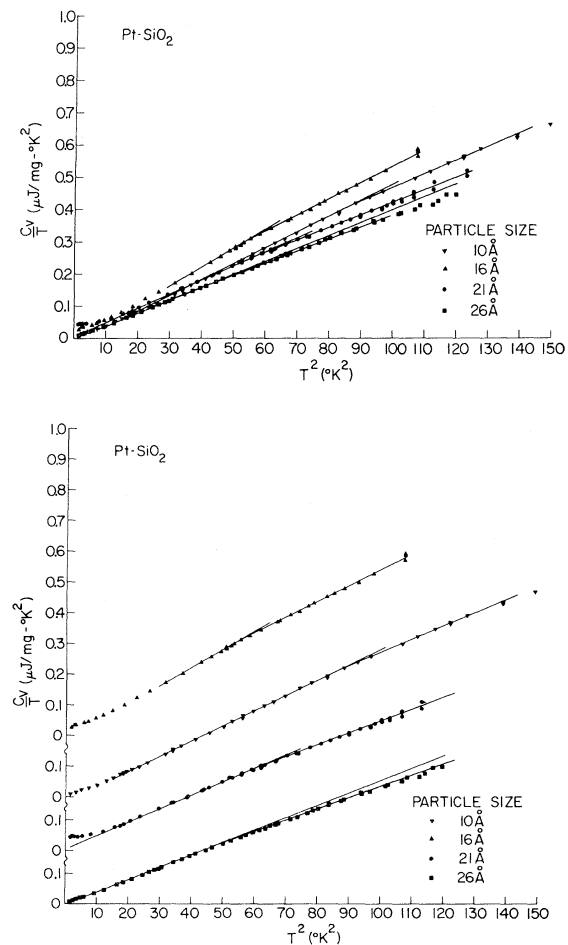


FIG. 3. (a) C/T vs T^2 of the four Pt-SiO₂ samples. Data appear to follow the simple relationship $C/T = \gamma + \beta T^2$, with a change in the slope, β , as the temperature is increased. This lack of T^5 dependence at low temperatures as predicted by DMS (Ref. 5) for symplectic small metal particles (Pt has a large spin-orbit coupling parameter η) was due to the obscuring enhancement in C_{SiO_2} discussed in the text. (b) Same as Fig. 3(a), with y axis broken to show detail.

including the 0.33-mm (13-mil) Al_2O_3 substrate for the films as part of the addenda.

IV. EXPERIMENTAL RESULTS AND DISCUSSION

The low-temperature heat capacity of the four Pt-SiO₂ films is shown both in Figs. 3(a) and 3(b), where Fig. 3(b) has a discontinuous ordinate to show detail at low temperatures. In order to examine the effect of small size on the heat capacity of the Pt metal, Fig. 4 shows the data for each film with the expected bulk heat capacity subtracted,

$$\Delta C = C_{\text{data}} - AC_{\text{Pt}}^{\text{bulk}} - BC_{\text{SiO}_2}^{\text{bulk}}, \quad (6)$$

where A is the wt% of Pt in the film as determined by microprobe (Table II) and B is similarly for the SiO₂. The error bars in Fig. 4 are caused by the uncertainty in the microprobe results and also by the uncertainty in the heat capacity of SiO₂. What was used for $C_{\text{SiO}_2}^{\text{bulk}}$ was the published data of Flubacher *et al.*,¹⁵ who measured vitreous (amorphous) silica. Measurements in the present work on two vitreous SiO₂ films sputtered at 100 W show two differences from the Flubacher *et al.* data. The sputtered films have a linear term twice that of Flubacher's data, and a C that is $\sim 25\%$ lower at 10°K. These differences cause the greater part of the error estimates in Fig. 4. As will be seen in the discussion below, these error bars are unimportant to the conclusion.

As may be seen in Fig. 4, the net difference between the measured C and the predicted bulk C shows an enhancement, contrary to the predicted decrease of DMS in Fig. 1, at all temperatures ex-

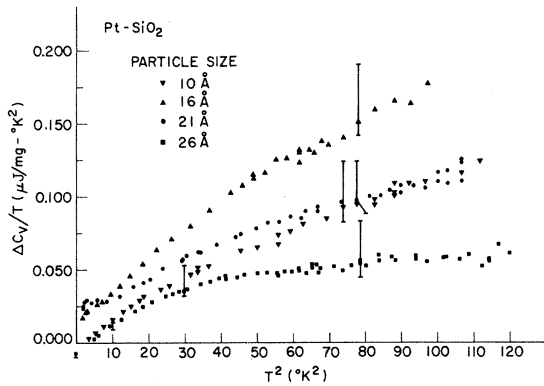


FIG. 4. $\Delta C/T$ vs T^2 ; the difference ΔC between the predicted C_{bulk} and C_{data} shows an enhancement over most of the temperature range. Note the extrapolated 26-Å particle sample point at $T=0$, showing a decrease in C_{data} vs C_{bulk} , i.e., a negative ΔC . Also, the change of slope present in Fig. 3 is seen to be missing; this is because this structure in the slope in Fig. 3 is caused by structure in C_{SiO_2} and has been subtracted away here.

cept below 2°K for the 26-Å particle sample. Thus, the discussion of the experimental results must deal with two different phenomena—the enhancement seen in most of the data and the decrease observed in the 26-Å particle sample at the lowest temperatures.

A. Enhancement

This enhancement was an enigma when first discovered, but a plausible explanation can be proposed based on Fig. 5. Since vitreous SiO₂ has three local modes, it was possible that microscopic inclusions (~ 20 Å) of a heavy metal could affect the strength of these modes. Indeed, the data in Fig. 5 show the typical structure of local-mode heat capacity. The heat capacity of an oscillator of a given frequency $\nu_E = k_B T_E/h$ is

$$\Delta C_{\text{Einstein}} = k_B x^2 e^x / (e^x - 1)^2, \quad x = h\nu_E / k_B T. \quad (7)$$

The usual technique¹⁹ in data reduction for assigning which Einstein oscillators are present, if any, is to plot $\ln(T^2 \Delta C)$ vs $1/T$. From Eq. (7) for $T < T_E$,

$$\Delta C_E \sim k_B x^2 e^{-x} \sim (k_B/T^2) e^{-T_E/T}. \quad (8)$$

Thus, this type of plot has a slope equal to $-T_E$. By considering Fig. 5, with $\Delta C/T^3$ vs T^2 plotted, there are two distinct types of behavior: the samples with particle sizes of 10 and 26 Å are similar at all temperatures, and samples with sizes 16 and 21 Å are almost identical below 3°K. Thus, plots of $\ln(T^2 \Delta C)$ vs $1/T$ are given in Fig. 6 for the 10, 16, and 26 Å samples.

From the straight-line behavior in Fig. 6, it is clear that there is indeed a low-temperature Ein-

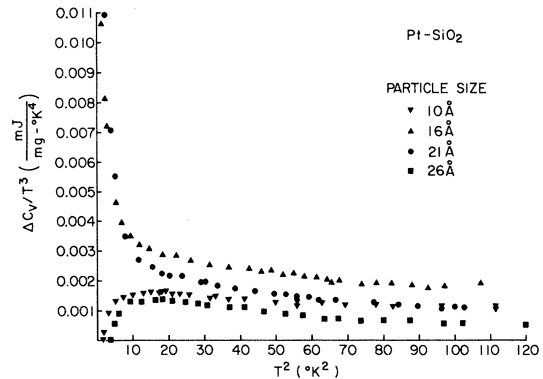


FIG. 5. $\Delta C/T^3$ vs T^2 . These curves show typical local mode behavior in their structure, with the peak in the 16- and 21-Å particle samples data indicating the presence of a lower-temperature mode than present in the 10- and 26-Å particle samples. Note that data with ΔC negative occurred for the 26-Å particle sample below $T^2 = 10^\circ\text{K}^2$ and is detailed in Table III.

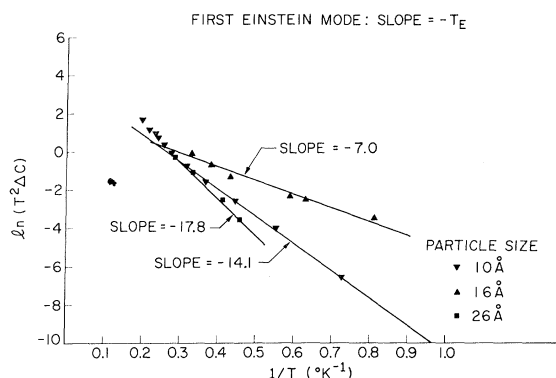


FIG. 6. From Eq. (8), a plot of $\ln(T^2 \Delta C)$ vs $1/T$ has a slope giving the negative of an Einstein local mode oscillator frequency, if one is present. As demonstrated by this figure, local modes appear to be present at the indicated temperatures.

stein mode present that is causing this enhanced heat capacity of Fig. 4. Figure 7 subtracts off the first Einstein mode discovered via Fig. 6 from ΔC and plots the remainder ΔC^* again for the two types of samples. Figure 7 shows that there is also a second Einstein mode present in ΔC . Further determination of modes is prohibited by the small size of the remainder ΔC^{**} and uncertainties in the subtraction of the first two modes.

However, Figs. 6 and 7 give rather conclusive indication that at least two low-temperature modes are present in the heat capacity ΔC , the difference between the data and the bulk C of the same amount of Pt and SiO_2 . The similarity of the Einstein temperatures of these modes with those of vitreous SiO_2 (13 and 32°K)¹⁵ further indicates that the source of these modes is the Pt particles increasing the strength of the modes of the surrounding silica. The enhancement in the 32°K silica mode is quite small, <0.3% change, while the 13°K mode is enhanced by a factor of 3 in the 10 Å sam-

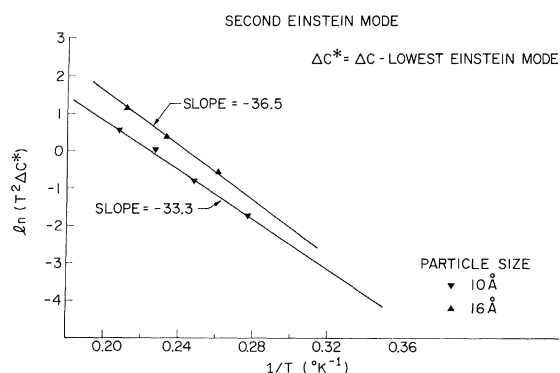


FIG. 7. By subtracting the Einstein oscillators obtained via Fig. 6, the remaining low-temperature data indicate additional Einstein modes as indicated.

ple and enhanced a factor of 1.2 and shifted down to 7°K in the 16 Å sample.

The exact mechanism for why the SiO_2 modes are enhanced is no clearer than why pure vitreous SiO_2 has local modes. In a review paper,²⁰ Lead-better states that the low-temperature Einstein modes of silica are quite likely localized vibrations associated with structural defects of some form. Thus, it is at least plausible that small particle inclusions could be expected to increase these structural defects as implied by the heat-capacity data.

B. Decrease

This effect on the structural defects would of course be greatest for the samples with the greatest number of particles per unit volume. This correlates with the density of the films; from Table II, then, the measured densities imply in a qualitative way that the films with the 10 and 26 Å particles would have the least enhancement (as they do) since their densities are lowest. In fact, from Fig. 5, it appears that both these samples would have negative ΔC 's at low temperatures. Unfortunately, at the lowest temperature reachable (1.25°K) only the 26 Å sample has a negative ΔC . This is of course just what is desired in order to show a decrease in C^{el} , as predicted by Kubo and DMS.

Shown in Table III is the derived C^{el}/T for the 26-Å Pt- SiO_2 sample at the lowest temperatures. This is derived by subtracting from the data the expected bulk contributions just as in Eq. (6) above, with two changes. Only the lattice contribution of Pt is used, of course, and a small correction term due to the enhanced lowest-temperature Einstein

TABLE III. Sample No. 3 Pt- SiO_2 C^{el} for Pt small particles.

$\frac{C_{\text{data}}}{T} \left(\frac{\mu\text{J}}{\text{mg}^\circ\text{K}^2} \right)$	T^2 ($^\circ\text{K}^2$)	$\frac{C^{el}}{T} \left(\frac{\mu\text{J}}{\text{mg}^\circ\text{K}^2} \right)^a$
0.00 976	1.57	0.00 514 (0.4%) ^b
0.00 956	1.575	0.00 493 (0.4%)
0.00 977	1.582	0.00 514 (0.4%)
0.01 013	1.737	0.00 525 (0.6%)
0.01 214	2.276	0.00 64 (2%)
0.01 56	3.446	0.00 768 (7%)
0.01 656	3.751	0.00 799 (7%)
0.02 007	4.841	0.00 894 (13%)

^a $C^{el}/T = C_{\text{data}}/T - C_{\text{Pt}}^{\text{lattice}}/T - C_{\text{SiO}_2}/T - C_{\text{Einstein mode}}^{\text{lowest}}/T$. This can be compared to the bulk value of $C^{el}/T (\mu\text{J}/\text{mg}^\circ\text{K}^2) = 0.0094$.

^b Figures in parentheses are the % of the data that is subtracted for the lowest Einstein mode in order to arrive at the derived C^{el}/T .

mode in the silica is also subtracted. As can be seen in Table III, this last correction is negligible at the lowest temperatures.

Since $C_{\text{bulk Pt}}^{\text{el}}/T$ is equal to 0.0094 in the units of Table III,²¹ these data clearly imply a decrease in the electronic heat capacity of small metal particles. The possible error in these derived $C_{\text{small Pt}}^{\text{el}}/T$ values comes mostly from two sources: the uncertainty of $\pm 4\%$ in the microprobe results for the amount of Pt present in the film, and the size of the SiO_2 contribution at these low temperatures. The microprobe uncertainty can change the derived $C_{\text{small Pt}}^{\text{el}}/T$ values at the lowest temperatures by at most 20%. This still implies a decrease in $C_{\text{bulk Pt}}^{\text{el}}/T$ of at least 35% at 1.25°K.

The major objection to assigning these observed decreases in the expected low-temperature heat capacity of the 26-Å particle sample to small size effects in C^{el} comes from possible effects in the insulating matrix of SiO_2 . These fall into two categories: whether the inclusion of small metal particles (or isolated atoms undetected by TEM) can decrease C_{SiO_2} at low temperatures; and whether the correct numbers for $C_{\text{SiO}_2}^{\text{bulk}}$ have been used to arrive at Table III.

The uncertainty in $C_{\text{SiO}_2}^{\text{bulk}}$ is indeed sizable, but only in a direction that decreases the apparent C^{el} measured in Table III. This is because the data of Flubacher¹⁵ for $C_{\text{SiO}_2}^{\text{bulk}}$ which were used [Eq. (6)] to calculate ΔC is in fact smaller at low temperatures than $C_{\text{SiO}_2}^{\text{bulk}}$ measured on two sputtered films in this experiment. The use of Flubacher's data is conservative; the use of the average $C_{\text{SiO}_2}^{\text{bulk}}$ at 1.25°K of the two sputtered films would imply a decrease in $C_{\text{bulk Pt}}^{\text{el}}/T$ of 75%, versus the 45% figure in Table III using Flubacher's¹⁵ data.

The other uncertainty in C_{SiO_2} is whether atomic or larger inclusions of Pt can decrease the heat capacity of SiO_2 and thus account for the observed decrease in Table III. The direct opposite is in fact to be expected. We have seen above that in the specific case treated in this work, Pt in SiO_2 , that low-frequency Einstein modes in the host lattice have been augmented markedly by heavy metal inclusions. In the more general case of a heavy metal atom in a host lattice, both experimental²² and theoretical work²³ indicate that low-frequency modes associated with the isolated heavy metal impurity increases the low-temperature heat capacity of the host lattice with inclusions over a pure specimen of the host material. This increase is small at low temperatures, $T \ll (\hbar/k_B)\omega_0$, where ω_0 is the resonant frequency of the isolated heavy impurity atom. For Pt in SiO_2 the resonant frequency of any isolated metal atom would be well

above 2°K and thus this effect can be ignored.

In fact, in order to explain the apparent decrease in C^{el}/T in Table III by a decrease in C_{SiO_2} requires that the host SiO_2 lattice heat capacity be slightly negative. Effects in the Pt lattice likewise would tend to decrease the apparent C^{el}/T , since the surfaces of the small metal particles tend to have less lattice binding, therefore have lower Θ_D 's and higher C^{lattice} 's. However, as discussed in Sec. I above, the lattice contribution of Pt at low temperatures is small, and is, in fact, only 4% of C_{Pt} at 1.25°K.

Thus, decreases in C^{lattice} in either or both Pt and SiO_2 are not possible explanations for the observed decreases in the low-temperature heat capacity of sample No. 3 of this work. As a working hypothesis, then, the explanation for the observed decrease in the heat capacity of the composite Pt- SiO_2 sample No. 3 measured in this work is that, as shown in Table III, the electronic heat capacity of the 26-Å Pt particles has decreased relative to $C_{\text{bulk Pt}}^{\text{el}}$, as predicted by Kubo⁴ and by DMS.⁵

V. CONCLUSIONS

This experiment has shown that cosputtering a metal with an insulator is a fruitful and flexible method of preparing isolated small metal particles. Cosputtered Pt- SiO_2 samples were measured using a small sample calorimeter and showed, on one sample, a definite decrease in the electronic heat capacity. Also discovered was an important increase in the strength of the two low temperature Einstein oscillators (at 13 and 32°K) in SiO_2 caused by the Pt particle inclusions. In order to further investigate size effects in the electronic heat capacity of small metal particles, three courses of action may be taken. The heat capacity may be measured to lower temperatures. The contribution of the amorphous SiO_2 at low temperatures may be investigated more thoroughly to enable a definite value of $C_{\text{SiO}_2}^{\text{bulk}}$ to be subtracted. A different insulator than SiO_2 may be used (not Al_2O_3)^{13,14} which has a smaller linear term at low temperature and less important Einstein modes, e.g., GeO_2 .²⁰

ACKNOWLEDGMENTS

The author wishes to acknowledge gratefully the work and assistance of Dr. Benjamin Abeles of RCA in the early stages of the sputtering work, when the vagaries of sputtered Al_2O_3 were first being revealed. Also, the author wishes to thank Dr. T. H. Geballe and Dr. C. N. King for helpful suggestions throughout the course of this work.

- *Research was supported partly by the AFOSR, Air Force Systems Command, USAF, under Grant No. AFOSR 73-2435 B and partly by the NSF.
- ¹R. E. Schwall, R. E. Howard, and G. R. Stewart, *Rev. Sci. Instrum.* **46**, 77 (1975).
- ²H. Fröhlich, *Physica (Utr.)* **4**, 406 (1937).
- ³R. Kubo, *J. Phys. Soc. Jpn.* **17**, 975 (1962).
- ⁴R. Kubo, *Livre de Jubile l'honneur du Professor A. Kastler* (University Press of France, Paris, 1969), p. 325.
- ⁵R. Denton, B. Muhlschlegel, and D. J. Scalapino, *Phys. Rev. Lett.* **26**, 707 (1971).
- ⁶V. Novotny, P. P. M. Meincke, and J. H. P. Watson, *Phys. Rev. Lett.* **28**, 901 (1972).
- ⁷V. Novotny and P. P. M. Meincke, *Phys. Rev. B* **8**, 4186 (1973).
- ⁸For a good review, see C. E. Porter, *Statistical Theories of Spectra: Fluctuations* (Academic, New York, 1965).
- ⁹M. L. Mehta, *Random Matrices and the Statistical Theory of Energy Levels* (Academic, New York, 1967), p. 9.
- ¹⁰E. P. Wigner, ORNL Report No. 2309, 1957 (unpublished); in Ref. 8, p. 199.
- ¹¹F. J. Dyson, *J. Math. Phys.* **3**, 140 (1962).
- ¹²R. Denton, Ph.D. dissertation (University of California, Santa Barbara, 1971) (unpublished).
- ¹³G. R. Stewart and B. Abeles, *Bull. Am. Phys. Soc.* **19**, 347 (1974).
- ¹⁴G. R. Stewart and B. Abeles (unpublished).
- ¹⁵P. Flubacher *et al.*, *J. Phys. Chem. Solids* **12**, 53 (1959).
- ¹⁶R. C. Zeller and R. O. Pohl, *Phys. Rev. B* **4**, 2029 (1971).
- ¹⁷J. W. Jeffrey, *Methods in X-Ray Crystallography* (Academic, London, 1971), p. 83.
- ¹⁸R. Bachmann *et al.*, *Rev. Sci. Instrum.* **43**, 205 (1972).
- ¹⁹C. N. King, in *Proceedings of the Thirteenth International Conference on Low Temperature Physics, Boulder, Colo., 1972*, edited by R. H. Ropschot and K. D. Timmerhaus (University of Colorado Press, Boulder, Colo., 1973), Vol. III, p. 411.
- ²⁰A. J. Leadbetter, *Phys. Chem. Glasses* **9**, 1 (1968).
- ²¹W. T. Berg, *J. Phys. Chem. Solids* **30**, 69 (1969).
- ²²W. M. Hartmann, H. V. Culbert, and R. P. Huebner, *Phys. Rev. B* **1**, 1486 (1970).
- ²³Yu. Kagan and Ya. Iosilevskii, *Zh. Eksp. Teor. Fiz.* **45**, 819 (1963) [*Sov. Phys.-JETP* **18**, 562 (1964)].